Pressure induced B3–B1 structural phase transformation and elastic properties of semi-magnetic semiconductors $Zn_{1-x}M_xSe$ (M = Mn, Fe and Cd)

2008 J. Phys.: Condens. Matter 20 075204

(http://iopscience.iop.org/0953-8984/20/7/075204)

J. Phys.: Condens. Matter **20** (2008) 075204 (10pp) doi:10.1088/0953-8984/20/7/075204

Pressure induced B3–B1 structural phase transformation and elastic properties of semi-magnetic semiconductors $Zn_{1-x}M_xSe$ (M = Mn, Fe and Cd)

Dinesh Varshney[1,3], **U Sharma**[1] **and N Kaurav**[2,4]

[1] School of Physics, Vigyan Bhawan, Devi Ahilya University, Khandwa Road Campus, Indore 452001, India
[2] Department of Physics, National Dong Hwa University, Hualien 97401, Taiwan

E-mail: vdinesh33@rediffmail.com

Received 30 August 2007, in final form 19 December 2007
Published 25 January 2008
Online at stacks.iop.org/JPhysCM/20/075204

Abstract

We have employed an effective interionic interaction potential approach to describe the high-pressure phase transformation and mechanical properties of diluted magnetic semiconductors $Zn_{1-x}M_xSe$ (M = Mn, Fe and Cd). This potential consists of the long-range Coulomb and three-body interactions (TBI) and the Hafemeister and Flygare type short-range overlap repulsion extended up to the second neighbour ions and the van der Waals (vdW) interaction. Our calculated results have revealed reasonably good agreement with the available experimental data on the phase transition pressures (P_t = 10, 12, 10 GPa) and the elastic properties of $Zn_{1-x}M_xSe$. The equation of state curves (plotted between $V(P)/V(0)$ and pressure) for both the zincblende (B3) and rocksalt (B1) structures obtained by us are in fairly good agreement with the experimental results. The calculated values of the volume collapses ($\Delta V(P)/V(0)$) are also closer to the observed data. Further, the variations of the second- and third-order elastic constants with pressure have followed a systematic trend, which are almost identical to those exhibited by the observed data measured for other compounds of this family.

1. Introduction

The structural phase transformations caused at high pressures in zincblende (ZB) structure (B3) compounds have attracted unprecedented interest in the recent past [1–3]. The spin splitting of the conduction bands in III–V and II–VI zincblende semiconductors (ZBS) have been determined by Chantis *et al* [2]. Also, the optical and vibrational modes of some of these compounds (HgTe, CdTe and ZnTe) have been studied by Belogorokhov *et al* [3]. The technological importance of these binary compounds has been exhibited by the diluted magnetic semiconductors (DMS) $A^{II}_{1-x}Mn_xC^{VI}$ [4], formed by replacing randomly a fraction of the cations in binary compound semiconductor alloys with magnetic ions. These DMS materials display interesting magnetic properties as well as the exchange interaction between the localized magnetic moment and the band electrons, resulting in a host of novel effects in comparison with the ternary nature of dilution like Mg or Be in AB compounds [5].

The phonons are believed to be an instructive probe for determining the structural aspects and Raman scattering [6] and they have been employed to study the zone-centre optical phonons in some of the DMS materials at ambient pressure. These investigations reveal that $Cd_{1-x}Mn_xTe$ exhibits a two-mode behaviour, while $Zn_{1-x}Mn_xTe$ displays an intermediate-mode behaviour in the phonon dispersion curves [7]. Earlier, Arora and co-workers [8] made a detailed Raman scattering investigation of zone-centre optical phonons and the intermediate high-pressure phase transition in $Zn_{1-x}Mn_xSe$. Under hydrostatic pressure, the mixed crystals

[3] Author to whom any correspondence should be addressed.
[4] On leave from: Department of Physics, Institute of Science and Laboratory Education, IPSA, Rajendra Nagar, Indore 452012, India.

undergo a high-pressure phase transition between 28 and 52 kbar depending on the composition.

Energy-dispersive x-ray-diffraction (EDXD) is a powerful technique for studying the pressure-induced transition of $Zn_{1-x}M_xSe$ bulk samples with M = Mn, Fe and Cd [9, 10]. These results show that phase transitions occur from the ZB structure (B3) to rocksalt (RS) structure (B1) under the application of hydrostatic pressure. It is interesting to note that pure ZnSe undergoes a transition from the B3 to B1 structure at about 13 GPa [11]. In particular, Lin *et al* [9] have argued that this reduction of transition pressure in comparison to the binary compounds can be seen in terms of fractional volume change at the B3 $\rightarrow$ B1 phase transition pressures.

Theoretical studies of structural mechanical and vibrational properties of II–VI, III–V and other doped semiconductors under pressure are now routinely being performed by means of *ab initio* calculations. The accuracy of total energies obtained within the local density approximation is in many cases sufficient to predict which structure, at a given pressure, has the lowest free energy, although most calculations still refer to zero temperature. Furthermore, by comparing the free energies of various guessed crystal structures, new *ab initio* molecular dynamics methods allow a better determination of the structures and understanding of transformation mechanisms and perform the structural optimizations. Despite the rapid development of computational techniques, the nature of interatomic forces is not well understood in these materials and phenomenological lattice dynamical models that take into account various interaction energies for the determination of stable structure and cover chemical trends in the atomic characteristics are important.

Theoretical prediction of the phase transition in II–VI semiconductors has been done by means of the lattice model [12] and accurate first-principles calculations [2, 13]. The reported theoretical values for the B3–B1 transition pressure in ZnSe are 4.4 [13] and 28.2 [12] GPa. Powder crystal of ZnSe studied by Raman scattering spectroscopy reveals a phase-transition pressure of 14.4 GPa, attributed to the ZB to RS structure transformation [9]. Energy-dispersive x-ray-diffraction (EDXD) is used to study the pressure-induced transitions for doped ZnSe and the P_ts of $Zn_{0.84}Fe_{0.16}Se$, $Zn_{0.76}Mn_{0.24}Se$ and $Zn_{0.9}Cd_{0.1}Se$ are 11.4, 9.6 and 9.5 GPa, respectively [10]. The doping dependence is further investigated and it is noticed that $Zn_{1-x}Mn_xSe$ shows structural transitions from the ZB (B3) to the RS phase (B1). The pressure-induced phase transition pressures occur at 13.1, 12.4, 12.0, 11.8 and 9.6 GPa for $Zn_{0.984}Mn_{0.016}Se$, $Zn_{0.974}Mn_{0.026}Se$, $Zn_{0.947}Mn_{0.053}Se$, $Zn_{0.93}Mn_{0.07}Se$ and $Zn_{0.76}Mn_{0.24}Se$, respectively [10]. In addition, Chelikowsky [14] and Zhang and Choen [15] used the pseudopotential total energy (PTE) method to compute the phase transition pressures for all the III–V compound semiconductors and stressed that the RS structure is preferred as the ionicity (or charge transfer) is increased in these materials. This suggestion motivated us to employ the concept of charge transfer effects [16–18] in DMS materials.

Usually, the mechanical properties of crystalline solids provide valuable information about their interatomic forces as well as their mechanical properties. Among these are the higher-order elastic constants and the pressure derivatives of second-order elastic constants (SOECs). Sörgel and Scherz [19] have performed first-principles calculations of cubic ZnSe and ZnTe crystals to deduce the SEOCs and third-order elastic constants (TOECs) under uniaxial strain, as well as under biaxial strain. Moreover, the ultrasonic transit time measurements [20] near room temperature in $Zn_{1-x}Mn_xSe$ (x = 0.0–0.53) reveal that increase in Mn doping concentration reduces the SEOCs and holds hexagonal symmetry.

The modelling of lattice models in binary semiconducting compounds is a complicated task and, in many instances, must be guided by experimental evidence of the low degree of freedom in order to obtain a correct minimal model which will capture the observed effect and will make useful predictions. First-principles density functional theory and microscopic tight binding models, as well as effective Hamiltonian models, have been used successfully to address the electronic, magnetic and structural ground state properties. On the other hand, phenomenological lattice models [16–18] have proved very successful in obtaining a qualitative and quantitative understanding with proper parametrization. Despite their successes, the basic nature of these interatomic potentials is such that they are inadequate to reveal a realistic picture of the interaction mechanism in ionic solids. The inadequacy of the two-body interaction is clearly indicated by its failure to explain the Cauchy violations in ionic crystals [16–18, 21, 22]. An acceptable explanation of these violations [22] was given by Löwdin [16] and Lundqvist [17] in terms of three-body interactions (TBI), which have their origin in the non-orthogonality of electron wave functions [16, 17] or charge transfer (or exchange of charge) between adjacent ions [18].

In the present paper, we have incorporated the effects of the TBI, which arise from the charge transfer mechanism [18] caused by the deformation (or exchange of small charge) of the electron shells of the overlapping ions. Besides TBI effects, we have included the van der Waals (vdW) interaction effects [22]. The overlap repulsion is expressed by the Hafemeister and Flygare [23] type interactions extended up to the second neighbour ions. The estimation of the vdW coefficients has been done by following the Slater–Kirkwood variational method with the idea that both the ions are polarizable.

The phase transition pressures, the volume collapses and the mechanical properties (higher-order elastic constants) are obtained from the present model, which incorporates the long-range Coulomb and TBI effects and the short-range vdW attraction and the overlap repulsive interactions operative up to the second neighbour ions within the Hafemeister and Flygare framework. The computed results have been compared with the available experimental data and are presented in the subsequent sections along with a brief description of the present TBI model as illustrated in appendix A. Comparison of the phase transition pressures, the volume collapses and the mechanical properties (higher-order elastic constants) in diluted magnetic II–VI semiconductors has allowed us to attain useful insights about the relative strength of elastic and thermal properties. Theoretical results are compared and discussed in

section 3 with the existing first-principles, experimental and predicted data with concluding remarks presented in section 4.

2. Three-body potential model computational approach

An application of pressure on a crystal causes a decrease in its volume leading to the charge transfer (or three-body) interaction due to the deformation of the electron shells of the adjacent ions [16–18] (please see appendix A for details). The effect of charge transfer has been incorporated in the Gibbs free energy ($G = U + PV - TS$). Here, U is the internal energy, which at $T = 0$ K is equivalent to the lattice (or cohesive) energy. S is the vibrational entropy, P is the pressure and V the volume. At $T = 0$ K, the Gibbs free energy is given by [18]

$$G_{\mathrm{B3}}(r) = U_{\mathrm{B3}}(r) + PV(= 3.08r^3) \tag{1}$$

for the ZB (B3, real) structure and

$$G_{\mathrm{B1}}(r') = U_{\mathrm{B1}}(r') + PV(= 2.0r'^3) \tag{2}$$

for the RS (B1, hypothetical) structure. Here the abbreviations $U_{\mathrm{B3}}(r)$ and $U_{\mathrm{B1}}(r')$ stand for cohesive energies for the ZB (B3) and RS (B1) structure, respectively. They consist of the long-range Coulomb and three-body interaction and the short-range vdW and overlap repulsive interactions effective up to the second neighbour ions. Their relevant expressions are written as [18]

$$\begin{aligned} U_{\mathrm{B3}} &= (-\alpha_M Ze^2/r)[Z + 2nf(r)] - Cr^{-6} - Dr^{-8} \\ &\quad + nb\beta_{ij}\exp[(r_i + r_j - r_{ij})/\rho] \\ &\quad + (n'b/2)[\beta_{ii}\exp((2r_i - kr_{ij})/\rho) \\ &\quad + \beta_{jj}\exp((2r_j - kr_{ij})/\rho)] \end{aligned} \tag{3}$$

$$\begin{aligned} U_{\mathrm{B1}} &= (-\alpha'_M Ze^2/r')[Z + 2mf(r')] - Cr'^{-6} - Dr'^{-8} \\ &\quad + mb\beta_{ij}\exp[(r_i + r_j - r'_{ij})/\rho] \\ &\quad + (m'b/2)[\beta_{ii}\exp((2r_i - k'r'_{ii})/\rho) \\ &\quad + \beta_{jj}\exp((2r_j - k'r'_{jj})/\rho)] \end{aligned} \tag{4}$$

where α_{m} (α'_{m}) are the Madelung constants for B3 (B1) phases. $C(C')$ and $D(D')$ are the overall vdW coefficients for B3 (B1) phases, β_{ij} $(i, j = 1, 2)$ are the Pauling coefficients defined [22] as $\beta_{ij} = 1 + (Z_i/n_i) + (Z_j/n_j)$ with $Z_i(Z_j)$ and $n_i(n_j)$ as the valence and the number of electrons in the outermost orbit. Ze is the ionic charge and b (ρ) are the range (hardness) parameters. $r(r')$ are the nearest neighbour ion separations for ZB (RS) structures. The function $f(r)$ ($f(r')$) appearing in the second term of equation (3), (4) is a function that depends on the overlap integrals and measures the size differences between ions. Thus $f(r)$ is the three-body force parameter which takes into account the charge transfer effect and is expressed as $f(r) = f_0\exp(-r/\rho)$ [16, 18]. $r_i(r_j)$ are the ionic radii of ions $i(j)$. The charge transfer mechanism and the nature of the TBI is further illustrated in appendix A.

In order to demonstrate the effects of the charge transfer mechanism, we have computed the phase transition pressures, the associated volume collapses and the mechanical behaviour of the diluted magnetic semiconductor materials. The expressions for the TOECs and the pressure derivatives of the SOECs are presented in appendix B. The computed results are presented and discussed in the next section.

3. Results and discussion

Upon the application of pressure, new crystal phases appear in materials and the relative stability of two crystal structures needs an extremely accurate prediction. Theoretical studies of cohesive, structural and vibrational properties of semiconductors under pressure are now being accurately performed by means of *ab initio* calculations. Also, several empirical models suggest that the key for predicting relative structural energies is not absolute accuracy but the careful incorporation of the chemical trends in the atomic characteristics. The phenomenological models are interpretative rather than predictive of the stability of phases.

The present model has been applied to investigate the structural phase transitions and elastic properties in $Zn_{1-x}M_xSe$ (M = Mn, Cd and Fe) DMS materials. The phase transition pressure is determined by calculating the Gibbs free energy $G = U + PV - TS$ for the two phases. The Gibbs free energy becomes equal to the enthalpy $H = U + PV$ at $T = 0$ K. Usually high-pressure experiments result in huge pressures that causes a reduction of the material volume and the temperature variations will normally produce much smaller changes in the relative stabilities of different phases. It is thus physically meaningful to be concerned with the Gibbs free energy at zero temperature, which is the enthalpy H. At $T = 0$ K, the thermodynamically stable phase at pressure P is the one with the lowest enthalpy and the zero-temperature theory results in consistent agreement with experiment; however, the effects of finite temperature may be significant.

The effective interionic potential is constructed in a hierarchical and easily generalizable manner. We have studied such structural and elastic properties in an ordered way. The values of G or H have been computed using the values of the three model parameters, namely, range, hardness and the three-body parameter (b, ρ and $f(r)$), which have been evaluated from the equilibrium condition

$$\left|\frac{\mathrm{d}U(r)}{\mathrm{d}r}\right|_{r=r_0} = 0 \tag{5}$$

and the bulk modulus (B_{T}):

$$\left|\frac{\mathrm{d}^2U(r)}{\mathrm{d}r^2}\right|_{r=r_0} = (9kr_0)^{-1}B_{\mathrm{T}} \tag{6}$$

using the values of lattice constant ($2a$), bulk modulus (B_{T}) and the modified ionic charge. The values of the overall vdW coefficients C and D involved in equations (3) and (4) have been evaluated from the well-known Slater–Kirkwood variational method [24] and are listed in table 1. We consider the DMS materials $Zn_{1-x}M_xSe$ (M = Mn, Cd and Fe) to be partially ionic and understand their structural and elastic properties in an ordered way.

It is perhaps worth remarking that we have deduced the values of hardness b and range ρ and the three-body force parameter $f(r)$ from knowledge of the equilibrium distance and the bulk modulus following the equilibrium conditions for binary compounds [25]. The values of electronic polarizabilities for ZnSe, MnSe, FeSe and CdSe were taken

Table 1. The values of van der Waals (vdW) coefficients c_{ij} $(i, j = 1, 2)$ (in units of 10^{-60} erg cm^6), d_{ij} $(i, j = 1, 2)$ (in units of 10^{-76} erg cm^8) and overall vdW coefficients (C, D) for $Zn_{1-x}M_xSe$ semiconductors.

	vdW coefficients							
Solids	c_{11}	c_{12}	c_{22}	C	d_{11}	d_{12}	d_{22}	D
ZnSe	38.04	112.82	533.96	709.24	12.07	115.26	702.22	586.33
MnSe	74.84	178.14	533.96	1743.23	36.98	181.24	702.22	1409.63
FeSe	46.88	134.04	533.96	1403.97	18.87	135.75	702.22	1122.75
CdSe	12.83	231.34	533.96	1259.79	61.14	234.94	702.22	1082.45
$Zn_{0.83}Mn_{0.17}Se$	44.45	125.06	533.96	765.02	15.35	127.19	702.22	635.49
$Zn_{0.84}Fe_{0.16}Se$	39.62	116.46	533.96	725.70	13.06	118.72	702.22	600.57
$Zn_{0.9}Cd_{0.1}Se$	45.39	125.44	533.96	767.01	15.28	127.7	702.22	637.68

directly from experimental data [26] using the additivity rule and Lorentz factor $(4\pi/3)$. The values for the corresponding doped semiconductors have been evaluated using the virtual crystal approximation [27] and Vegard's law [28]. Knowledge of C and D, listed in table 1, enables us to estimate three model parameters for binary semiconductors XSe (X = Zn, Mn, Cd and Fe). We have obtained the model parameters (b, ρ and $f(r)$) for their mixed crystals $Zn_{1-x}M_xSe$ (M = Mn, Cd and Fe) using Vegard's law:

$$b(Zn_{1-x}M_xSe) = (1-x)b(ZnSe) + xb(MSe), \quad (7)$$

$$\rho(Zn_{1-x}M_xSe) = (1-x)\rho(ZnSe) + x\rho(MSe). \quad (8)$$

$$f(r)(Zn_{1-x}M_xSe) = (1-x)f(r)(ZnSe) + xf(r)(MSe). \quad (9)$$

The input data for undoped and doped semiconductors with their relevant references and the deduced model parameters from the knowledge of equilibrium distance (r_0), the bulk modulus (B_T) and the Cauchy violation ($C_{12} - C_{44}$) are given in table 2. In an attempt to reveal the structural phase transition of $Zn_{1-x}M_xSe$, we minimize the Gibb's free energies $G_{B3}(r)$ and $G_{B1}(r')$ for the equilibrium interatomic spacing (r_0) and (r_0'). Initially, the computations were done at $P = 0$ from equation (5) to know at what value of r, dG/dr becomes negative to positive for the stable phase, and subsequently we input various pressures to find r with a similar method. This enables one to obtain a pressure-dependent value of r. Any crystal is stable if the change in the Gibb's free energy is positive for all possible infinitesimal changes in structure, i.e. the first-order change in the enthalpy/Gibb's free energy must be zero and the second-order change must be positive.

The Gibb's free energy difference, $\Delta G\,(=G_{B3}(r) - G_{B1}(r'))$, has been plotted against pressure (P) in figures 1(a)–(c) by using the interionic potential as discussed above. The pressure corresponding to ΔG approaching zero is the phase transition pressure (P_t) (as indicted by arrows in these figures). At zero pressure, the B3 crystal phase is thermodynamically and mechanically stable, while the phase B1 is not. As pressure increases beyond the phase transition pressure (P_t), the B1 system becomes mechanically and thermodynamically stable and the ΔG values are negative compared to those of the B3 phase. Eventually, at a pressure higher than the theoretical thermodynamic transition pressure, the B3 structure becomes thermodynamically unstable, while the B1 phase remains stable from P_t up to pressures beyond 15 GPa.

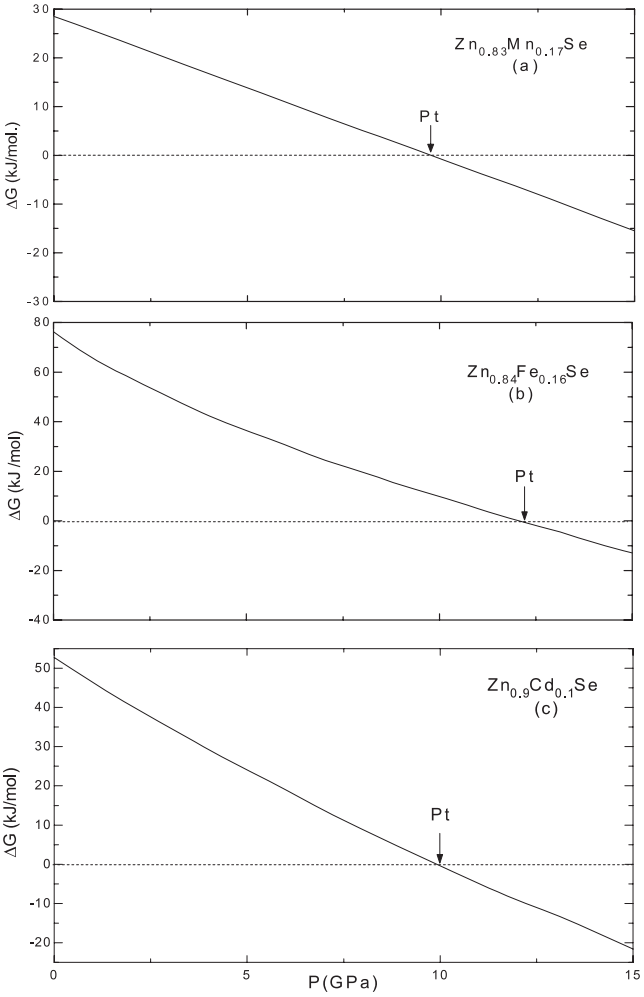

Figure 1. (a)–(c) Variation of Gibbs free energy difference $\Delta G(P)$ with pressure (P) for $Zn_{1-x}M_xSe$ (M = Mn, Fe and Cd).

In $Zn_xM_{1-x}Se$ (M = Mn, Fe and Cd) DMS the structural phase transition occurs from B3 to B1. Our theoretical results are in almost excellent agreement with the experimental [9, 10] data, as is seen from table 3. However, it is worthwhile pointing out that the uncertainties in the transition pressures in some cases are large as 10% or so. These deviations of 10% may be for the reasons discussed by Van Vechten [33] and arise due to the metastability in pressure experiments.

The values of the relative volumes $V(P)/V(0)$ associated with various compressions have also been calculated from the

Table 2. Crystal data and model parameters for $Zn_{1-x}M_xSe$ (M = Mn, Fe and Cd).

	Material parameters			Model parameters			
Solids	r_i (Å)	r_j (Å)	a (Å)	B_T (GPa)	b (10^{12} erg)	ρ (10^{-1} Å)	$f(r)(10^{-3})$
ZnSe	0.83[a]	1.94[a]	2.835[b]	62.37[d]	1.51	3.44	7.29
MnSe	0.8[a]	1.94[a]	2.556[b]	17.16[d]	1.48	6.7	17.5
FeSe	0.76[a]	1.94[a]	2.909[c]	58.85[c]	0.47	4.98	12
CdSe	1.03[a]	1.94[a]	3.04[c]	43.33[c]	0.88	4.4	7.32
$Zn_{0.83}Mn_{0.17}Se$					1.48	3.93	9.03
$Zn_{0.84}Fe_{0.16}Se$					1.34	3.68	8.03
$Zn_{0.9}Cd_{0.1}Se$					1.44	3.53	7.29

[a] Reference [29].
[b] Reference [30].
[c] Reference [31].
[d] Reference [32].

Table 3. Calculated (experimental) transition pressures and volume collapses in $Zn_{1-x}M_xSe$ (M = Mn, Fe and Cd).

Compounds	Transition pressure P_t (GPa)	Volume collapses (%)
$Zn_{0.83}Mn_{0.17}Se$	10(10.0)[a]	11.7(12.5)[a]
$Zn_{0.84}Fe_{x0.16}Se$	12(11.4 ± 0.5)[b]	7.4(13.4)[b]
$Zn_{0.9}Cd_{0.1}Se$	10(9.5 ± 0.3)[b]	10(16.1)[b]

[a] Reference [10].
[b] Reference [9].

Murnaghan equation of state [34]:

$$\frac{V}{V_0} = \left(1 + \frac{B'}{B_0}P\right)^{-\frac{1}{B'}}, \tag{10}$$

with V_0 as the unit cell volume at ambient conditions. The estimated values of the pressure-dependent radii $r(P)$ for both structures (B3 and B1) have been used to compute the values of $V(P)/V(0)$ and plotted against the pressure (P) as illustrated in figures 2(a)–(c) for $Zn_xM_{1-x}Se$ (M = Mn, Fe and Cd). It is noticed from these plots that our approach has predicted correctly the relative stability of competitive crystal structures, as the value of ΔG are positive in both cases. The magnitude of the volume collapse ($-\Delta V(P_t)/V(0)$) at the transition pressure is obtained from the phase diagram and values are listed in table 3 and compared with the available experimental results [9, 10]. Our calculated values for $Zn_{0.83}Mn_{0.17}Se$ are in reasonably good agreement, but this is not the case in the other two materials, as is seen in table 3.

Initially, we have calculated the values of the model parameters {b, ρ and $f(r)$ } for pure ZnSe, MnSe, FeSe and CdSe and then applied Vegard's law for obtaining these parameters for $Zn_xM_{1-x}Se$ (M = Mn, Fe and Cd) at very low concentration $x = 0.17$ at which the basic crystal structure (or symmetry) does not change [27]. Thus, virtual crystal approximation [27] through Vegard's law [28] seems quite valid. Using these model parameters, we have evaluated the values of the SOECs and TOECs from their expressions given in appendix B at different pressures. The calculated values of these SOECs and TOECs are presented in figures 3(a)–(c) and 4(a)–(c), respectively. These results could not be compared due to the lack of experimental data and hence they will serve as a guide for experimental workers in future.

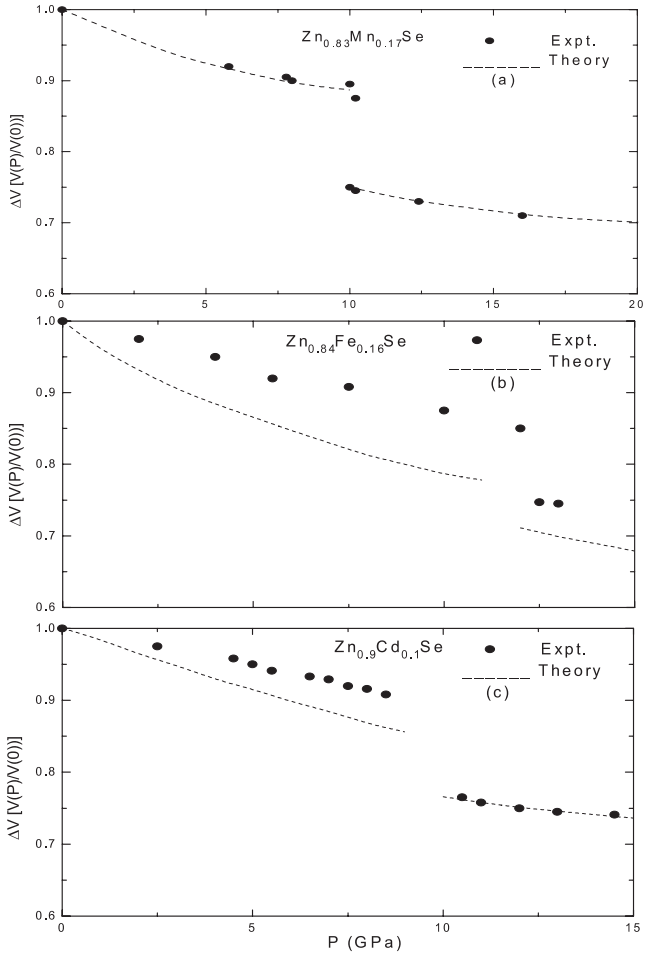

Figure 2. (a)–(c) Pressure–volume diagram of $Zn_{0.83}Mn_{0.17}Se$, $Zn_{0.84}Fe_{0.16}Se$ and $Zn_{0.9}Cd_{0.1}Se$.

It is noticed from figures 3(a)–(c) that the values of C_{11} and C_{12} increase linearly with increasing pressure. On the contrary, the values of C_{44} decrease almost linearly with increasing pressure. This feature is reasonable in view of the physical difference in the characteristics of C_{11}, C_{12} and C_{44}.

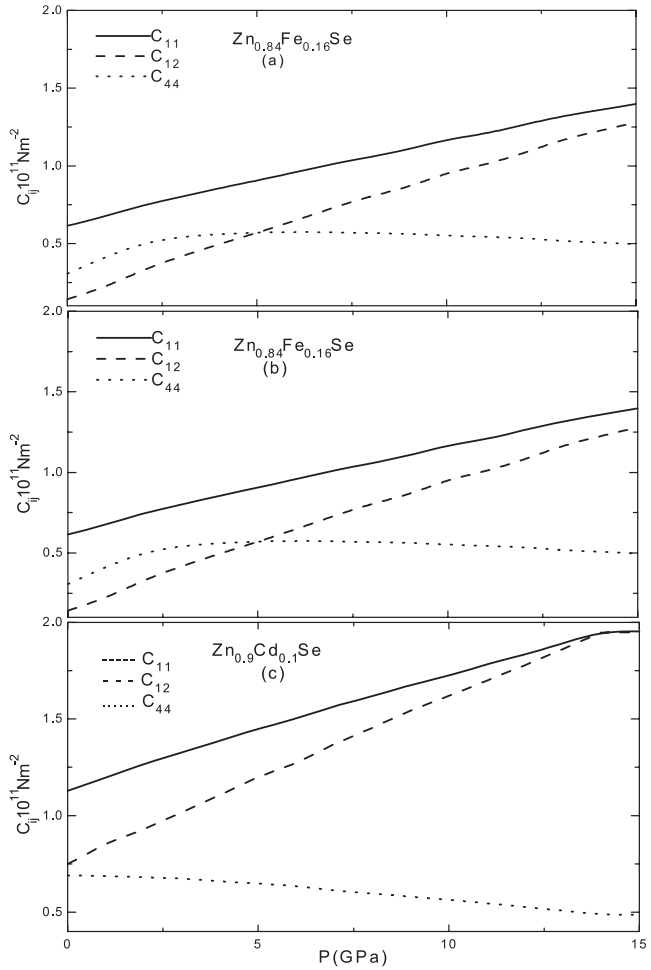

Figure 3. (a)–(c) Variation of second-order elastic constants with pressure.

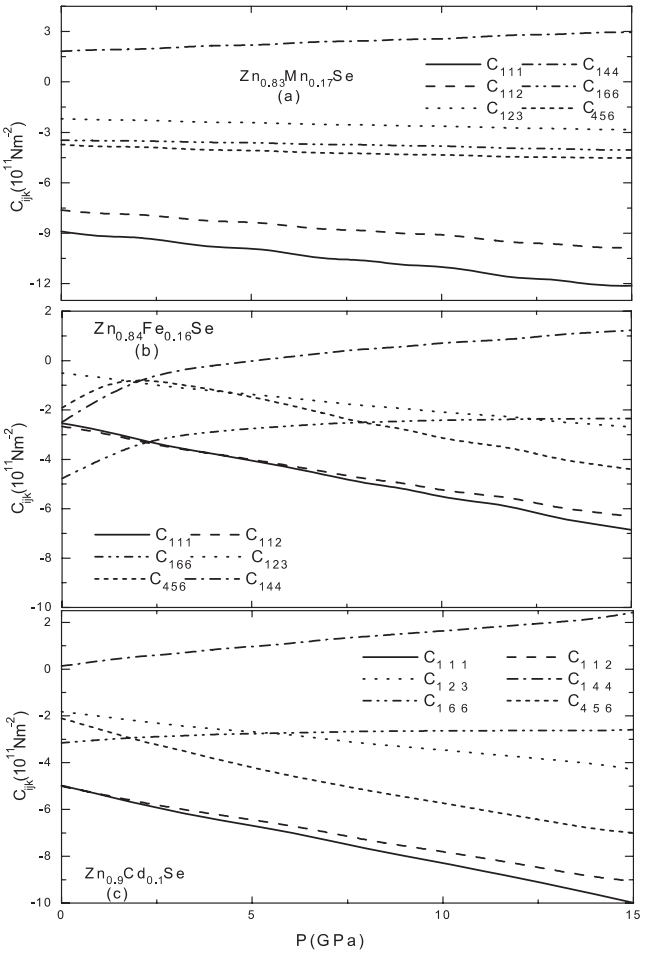

Figure 4. (a)–(c) Variation of third-order elastic constants with pressure.

A similar trend of variations of C_{11}, C_{12} and C_{44} with pressure has been revealed by Miller *et al* [35] from their measured values for HgTe and HgSe.

It seems worthwhile to mention that the Born criterion for a lattice to be in a mechanically stable state is that the elastic energy density must be a positive definite quadratic function of the strain. The stability of a cubic crystal is expressed in terms of the elastic constants [36]:

$$B_{\mathrm{T}} = (C_{11} + 2C_{12})/3 > 0, \tag{11}$$

$$C_{44} > 0, \tag{12}$$

$$\sigma = (C_{11} - C_{12})/2 > 0. \tag{13}$$

C_{ij} are the conventional elastic constants and B_{T} is the bulk modulus. The quantities C_{44} and σ are the shear and tetragonal moduli of a cubic crystal. Estimated values of the bulk modulus (182 GPa), shear modulus (30 GPa) and tetragonal moduli (87 GPa) for $Zn_{1-x}M_xSe$ are found to satisfy fairly well the above elastic stability criteria. In addition, Vukcevich [37] proposed a high-pressure stability criterion for ionic crystals, combining mechanical stability with minimum energy conditions. In accordance, the stable phase of the crystal is one in which the shear elastic constant (C_{44}) is nonzero (for mechanical stability) and which has the lowest potential energy among the mechanically stable lattices. Also, the pressure at which $C_{44} = 0$ (i.e. shear instability) indicates the upper bound for the transition. It is true that the agreement between the theoretical and experimental values of B_{T} is not of the desired degree but this might be because we have derived our expressions neglecting the thermal effects and assuming the overlap repulsion to be effective only up to the second nearest neighbour ions.

Furthermore, C_{44} is very small: the calculated value of $((4r_0^2/e^2)C_{44} + 0.556(Z + 8f(r_0)))$ is found to be negative so that $(A_2 - B_2)$ is negative. This suggests that these terms belong to an attractive interaction and possibly arise due to the vdW energy. The vdW energy converges quickly, but the overlap repulsion converges much more quickly. This means that the second neighbour forces are entirely due to the vdW interaction and the first neighbour forces are the results of the overlap repulsion and the vdW attraction between the nearest neighbours. However, at high pressures the short-range forces for these compounds increase significantly, which in turn is responsible for the change in the coordination number and phase transformation. Other than deriving the equations of state correctly from a lattice model approach and then analysing the variation of the short-range forces, at present we

Table 4. Pressure derivative of bulk modulus (B_T), shear modulus (C_{44}) and tetragonal modulus (σ) (in units of GPa) for $Zn_{1-x}M_xSe$ (M = Mn, Fe and Cd).

Compounds	dB_T/dP	dC_{44}/dP	$d\sigma/dP$
$Zn_{0.83}Mn_{0.17}Se$	$3.66(5.43 \pm 0.56)$[a]	0.34	−0.03
$Zn_{0.84}Fe_{0.16}Se$	$6.87(4.12 \pm 0.19)$[b]	11.2	−0.25
$Zn_{0.9}Cd_{0.1}Se$	$4.85(4.32 \pm 0.18)$[b]	1.0	0.48

[a] Reference [7].
[b] Reference [6].

have no direct means to understand the nature of interatomic interactions at high pressures.

We also intend to analyse the anharmonic properties of $Zn_{1-x}M_xSe$ compounds by computing the TOECs and the pressure derivatives of SOECs at zero pressure, described earlier [39]. The values of the pressure derivatives of SOECs ($d\sigma/dP$, dB_T/dP and dC_{44}/dP) for $Zn_{1-x}M_xSe$ are listed in table 4. A reasonably good agreement with available experimental results for dB_T/dP has been obtained in all the cases under consideration. Also, the variation of TOECs with pressure is shown in figure 4. It can be seen that the variation of third-order elastic constants with pressure points to the fact that the values of C_{111}, C_{112}, C_{123}, C_{166}, C_{456} are negative while that of C_{444} is positive as obtained from the effective interionic potential at zero pressure. Thus, we can say that in DMS the present effective interionic potential consistently explains the high-pressure and elastic behaviour of $Zn_{1-x}M_xSe$ semiconducting compounds.

Apart from the phase transition and the pressure dependence of SOECs, we have further estimated the Debye temperature (θ_D) from the present model approach using the expression [38]

$$\theta_D^3 = \frac{3.15}{8\pi}\left(\frac{h}{k_B}\right)^3\left(\frac{r}{M}\right)^{\frac{3}{2}}(C_{11}-C_{12})^{\frac{1}{2}} \times (C_{11}+C_{12}+2C_{44})^{\frac{1}{2}}C_{44}^{\frac{1}{2}}, \quad (14)$$

where M is the acoustic mass of the compounds and h and k_B are the Planck and Boltzmann constants, respectively. The values of θ_D are plotted in figure 5 as a function of pressure. It is inferred from the figure that θ_D decreases almost linearly with pressure for all the compounds and this feature may be attributed to the hardening of the lattice under pressure.

One can approximate this result with the definition of an *average* elastic constant as

$$C = \left(\frac{8\pi}{3.15}\right)^{\frac{2}{3}}\left(\frac{k_B}{h}\right)^2\left(\frac{M}{r}\right)\theta_D^2, \quad (15)$$

which in turn is calculated from the Debye temperature and allows us to correlate the Cauchy discrepancy in the elastic constant following

$$C^* = \frac{C_{12}-C_{44}}{C_{12}+C_{44}}, \quad (16)$$

at zero pressure. Figure 6 shows the variation of the *average* elastic constant (C) with the Cauchy discrepancy (C^*) for $Zn_{1-x}M_xSe$ compounds. It seems appropriate to mention that

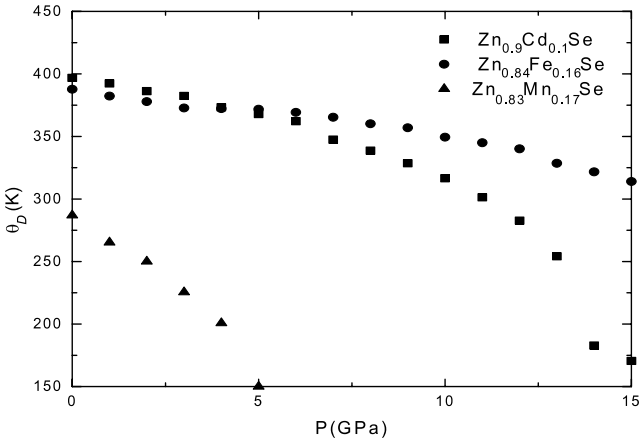

Figure 5. Variation of Debye temperature with pressure.

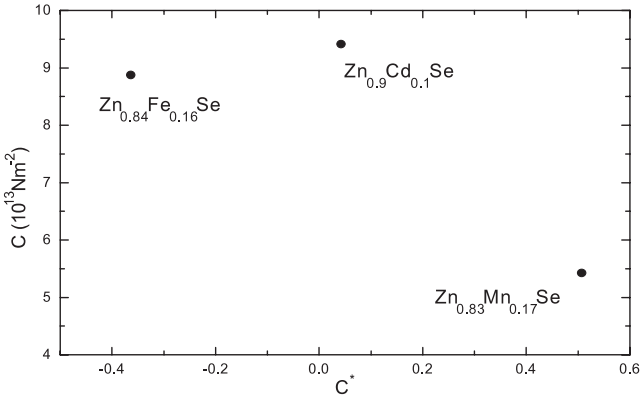

Figure 6. The average elastic constant (C) plotted as a function of the Cauchy discrepancy (C^*) for $Zn_{1-x}M_xSe$ compounds.

C_{44} is larger than C_{12}, which is consistent with the available experimental data on PbTe and SnTe [35]. However, we note that the DMS with ZB structure undergo the structural phase transition (B3 → B1) [39], the rare earth compounds [38], Y (Sc) antimonides (B1 → B2) [40] and alkaline earth chalcogenides [41] show a positive Cauchy deviation C^*.

4. Conclusion

At ambient pressures the DMS based on ZB II–VI compounds, such as (Zn, M)Se (M = Mn, Cd and Fe) crystallize in a B3 structure. As pressure is raised, one expects that these semiconductors show the ZB → RS structural phase transitions. To determine the most stable structure at finite pressure and temperature, the free energy $G = U + PV - TS$ should be used. Since the reported phase transformation for $A^{II}_{1-x}Mn_xC^{VI}$ group $A^{II}_{1-x}Mn_xC^{VI}$ DMS transformations are temperature independent, we neglect the last term and therefore calculated the pressure-induced elastic properties with stable ZB structures following the lattice models.

The computational methods for the determination of cohesive, structural and vibrational properties of semiconductors under pressure are now successfully being performed by means

of *ab initio* calculations such as the local density approximation and molecular dynamics methods. Despite the rapid development of computational techniques, the nature of interatomic forces in these materials is not well understood and lattice dynamical models are important in interpreting the chemical trends in structural stability. Realistic descriptions of alloys or semiconducting compounds need to take in to account various interactive forces when the lattice is strained and a balance of them to attain a stable structure depending upon the ionic or covalent nature.

We have formulated an effective interionic interaction potential for analysing the structural phase transition and mechanical (elastic) properties of some DMS materials. The values from the model parameters allow us to predict the experimental values available for the phase transition pressures and associated volume collapses in DMS materials $Zn_{1-x}M_xSe$ (M = Mn, Fe and Cd). A structural phase transition occurs at 10 GPa in $Zn_{0.83}Mn_{0.17}Se$, at 12 GPa in $Zn_{0.84}Fe_{x0.16}Se$, and at 10 GPa in $Zn_{0.9}Cd_{0.1}Se$, each into the RS-type structure. We stress that the vast volume discontinuity in pressure–volume phase diagram is ascribed in terms of the structural phase transition from ZS (B3) to RS (B1) structure. For these three compounds excellent agreement is found with the available data.

The remarkable feature revealed from the lattice models is that the vast volume discontinuity in the pressure–volume phase diagram is ascribed to the structural phase transition from ZB (B3) to RS (B1) structure. Precise first-principles calculations on structural properties are widely available, but we still feel that the lattice model calculations have their own importance. The ability of the effective interionic interaction potential (EIoIP) model to predict realistic cohesive properties such as the equilibrium volume, the bulk modulus, its derivative with pressure, the relative stability of crystal structures, and transition pressures and volumes is exemplified in terms of the screening of the effective Coulomb potential through the modified ionic charge (Z_m^2).

The calculations based on the lattice model also show the validity of the Born criterion. The second-order elastic constants C_{11} (C_{12}) increase with increase in pressure up to the phase transition pressure that supports high-pressure structural stability of these compounds. Further, C_{44} decreases linearly with the increase of pressure and does not tend to zero at the phase transition pressures, and this feature is in accordance with the first-order character of the transition. The consistency of the results obtained from the TBI potential arose because the electron-shell deformation, when the nearest neighbour ions overlap, is enhanced under pressure. This supports our view of a partially ionic character and a charge transfer. It is thus obvious from the overall results that the present TBI mechanism is adequately suited for a description of the phase transition phenomena and mechanical properties, and we stress that the TBI gives a realistic representation of interionic interaction capable of explaining the elastic behaviour. Our results are in good agreement with known theoretical and experimental works.

In conclusion, the proper incorporation of realistic physical parameters based on experimental observations will allow us to reveal a consistent high-pressure structural and mechanical behaviour of these compounds. Deviations appearing might be ascribed to the extension of the covalent and zero point motion effects. Efforts are being made to apply the many body interactions approach to describe the phase transition and volume collapses caused under pressure in other members of the DMS family.

Acknowledgment

Financial support from the Defence Research Development Organization (DRDO), New Delhi is thankfully acknowledged.

Appendix A

In order to understand the charge transfer mechanism and the nature of the TBI, let us consider the ions A, B and C designated by (lk), $(l'k')$ and $(l''k'')$, as shown in figure A.1, with l and k as the cell and basis indices. During the compression, the electron shells of A and C experience increased overlap and give rise to the transferred (or exchanged) charge:

$$\begin{aligned}\Delta g_k &= \pm Zef_k\{r(lk, l'k'')\},\\ &= \pm Zef_k(r)\end{aligned} \tag{A.1}$$

Ze being the ionic charge and $f_k(r)$, the function of the nearest neighbour separation $[r = r(lk, l'k'')]$ such that:

$$f_k(r) = (Z_k/Z)f(r),$$

with

$$Z = |Z_k| = |Z'_k|. \tag{A.2}$$

Thus, the ionic charge of A (or C) gets modified as:

$$\begin{aligned}Z_{mk}e &= Z_k e \pm nef_k(r(lk, l''k''))\\ &\approx \pm Z_k e[1 \pm (2n/Z)f(r(l'k', l''k''))]^{1/2}\end{aligned} \tag{A.3}$$

n being the number of nearest neighbours in equation (A.3) by expressing $(1 \pm n/Zf(r)) \approx (1 \pm (2n/Z)f(r))^{1/2}$. Thus, one writes

$$Z_{mk'}e = \pm Z'_k e[1 \pm (2n/Z)f(r(l'k', l'''k'''))]^{1/2} \tag{A.4}$$

in view of the smallness of $f(r)$.

Here, $(l'''k''')$ ion is the nearest neighbour of ion B and this is not shown in figure A.1. The modified Coulomb interaction potential can now be written as:

$$\begin{aligned}\Phi_{mc}(r(lk, l'k')) &= Z_{mk}Z_{mk'}e^2/|r(lk, l'k')|\\ &= (e^2/2)\sum_{lk}\sum_{l'k'} Z_{kk'}/|r(lk, l'k')| + e^2\sum_{lk}\sum_{l'k'}\sum_{l''k''} Z_k\\ &\quad \times f(r(lk, l''k''))Z_{k'}/|r(lk, l'k')|.\end{aligned} \tag{A.5}$$

The second term in equation (A.5) is the potential energy due to the interaction of transferred (or exchanged) charge $\Delta g_k = Zef(r(lk, l''k''))$ on the atom (lk) from the overlapping ions $(l''k'')$ of charge $Z'''_k e$ and separated by a distance $r(lk, l''k'')$: this interaction potential is termed the TBI potential since it depends on the coordinates of the three ions (lk), $(l'k')$ and $(l''k'')$.

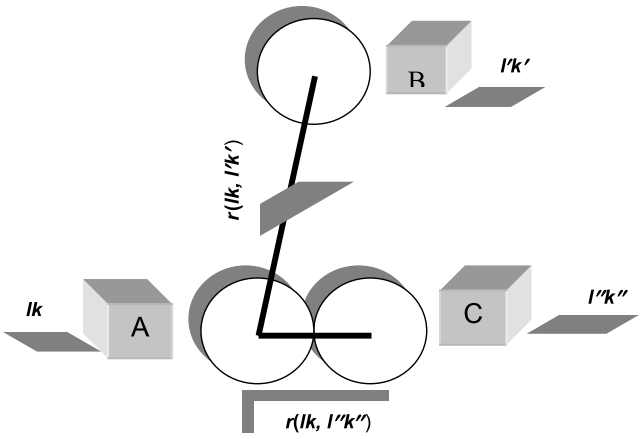

Figure A.1. Schematic representation of the TBI.

The charge transfer mechanism rests on the three-body parameter $f(r)$. $f(r_{ik})$ [or $f(r'_{ik})$] is dependent on the nearest neighbour separation (r) as [21]:

$$f(r) = f_0 \exp(-r/\rho) \tag{A.6}$$

with ρ as the range parameter defined previously.

Appendix B

We have also investigated the pressure variations of the SOECs and TOECs. The relevant expressions for the SOECs, TOECs and the pressure derivatives of SOECs are expressed [18] for the ZB structure as

$$C_{11} = L[0.2477Z(Z+8f(r_0)) + \tfrac{1}{3}(A_1+2B_1) + \tfrac{1}{2}(A_2+B_2) + 5.8243Zaf'(r_0)], \tag{B.1}$$

$$C_{12} = L[-2.6458Z(Z+8f(r_0)) + \tfrac{1}{3}(A_1-4B_1) + \tfrac{1}{4}(A_2-5B_2) + 5.8243Zaf'(r_0)], \tag{B.2}$$

$$C_{44} = L[-0.123Z(Z+8f(r_0)) + \tfrac{1}{3}(A_1+2B_1) + \tfrac{1}{4}(A_2+3B_2) - \tfrac{1}{3}\nabla(-7.53912Z(Z+8f(r_0)) + A_1 - B_1)] \tag{B.3}$$

$$C_{111} = L[0.5184g + \tfrac{1}{9}(C_1-6B_1-3A_1) + \tfrac{1}{4}(C_2-B_2-3A_2) - 2(B_1+B_1) - 9.9326Zg_1 + 2.522Zg_2], \tag{B.4}$$

$$C_{112} = L[0.3828g + \tfrac{1}{9}(C_1+3B_1-3A_1) + \tfrac{1}{8}(C_2+3B_2-3A_2) - 11.642Zg_1 + 2.522Zg_2] \tag{B.5}$$

$$C_{123} = L[6.1585g + \tfrac{1}{9}(C_1+3B_1-3A_1) - 12.5060Zg_1 + 2.5220Zg_2], \tag{B.6}$$

$$C_{144} = L\Big\{6.1585g + \tfrac{1}{9}(C_1+3B_1-3A_1) - 4.1681Zg_1 + 0.8407zg_2 + \nabla[-3.3507g - \tfrac{2}{9}C_1 + 13.5486Zg_1 - 1.681Zg_2] + \nabla^2\Big[-1.5637g + \frac{2}{3}A_1 - B_1) + \frac{C_1}{9} - 5.3138Zg_1 + 2.9350Zg_2\Big]\Big\} \tag{B.7}$$

$$C_{166} = L\Big\{-2.1392g + \tfrac{1}{9}(C_1-6B_1-3A_1) + \tfrac{1}{8}(C_2-5B_2-3A_2) - (B_1-B_2) - 4.168Zg_1 + 0.8407Zg_2 + \nabla[-8.3768g + \tfrac{2}{3}(A_1-A_2) - \tfrac{2}{9}C_1 + 13.5486Zg_1 - 1.6813Zg_2] + \nabla^2\Big[2.3527g + \frac{C_1}{9} - 5.3138Zg_1 + 2.9350Zg_2\Big]\Big\} \tag{B.8}$$

$$C_{456} = L\Big\{4.897g + \tfrac{1}{9}(C_1-6B_1-3A_1) - B_2 + \nabla[-5.0261g - \tfrac{1}{9}C_1] + \nabla^2[7.0580g + \tfrac{1}{3}C_1] + \nabla^3[-4.8008g + \tfrac{1}{3}(A_1-B_1) - \tfrac{1}{9}C_1]\Big\}. \tag{B.9}$$

Using the equilibrium condition

$$B_1 + B_2 = -1.261Z[Z + 8f(r)]. \tag{B.10}$$

In addition, the pressure derivatives of second-order elastic constants are expressed as

$$3\Omega\frac{\mathrm{d}B_\mathrm{T}}{\mathrm{d}p} = -[20.1788Z(Z+8f(r_0)) - 3(A_1+A_2) + 4(B_1+B_2) + 3(C_1+C_2) - 104.8433Zaf'(r_0) + 22.7008Za^2f''(r_0)] \tag{B.11}$$

$$2\Omega\frac{\mathrm{d}\sigma}{\mathrm{d}p} = -[-11.5756Z(Z+8f(r_0)) + 2(A_1-2B_1) + \tfrac{3}{2}A_2 - \tfrac{7}{2}B_2 + \tfrac{1}{4}C_2 + 37.5220Zaf'(r_0)] \tag{B.12}$$

and

$$\Omega\frac{\mathrm{d}C_{44}}{\mathrm{d}p} = -\Big\{\Big[0.4952Z(Z+8f(r_0)) + \frac{1}{3}(A_1-4B_1+C_1) + \tfrac{1}{4}(2A_2-6B_2+C_2) + 4.9667Zaf'(r_0) + 2.522Za^2f''(r_0)\Big] + \nabla[-17.5913Z(Z+8f(r_0)) + A_1 - B_2 - \tfrac{2}{3}C_1 + 40.6461Zaf'(r_0) - 5.044Za^2f''(r_0)] + \nabla^2\Big[3.1416Z(Z+8f(r_0)) + \frac{2}{3}(A_1-B_1) + \frac{C_1}{3} - 15.9412Zaf'(r_0) + 8.8052Za^2f''(r_0)\Big]\Big\}. \tag{B.13}$$

Various symbols appear in the earlier equations (5)–(16) which are associated with the crystal energy and have been defined below:

$$A_1 = A_{ij} = L'\left(\frac{\mathrm{d}^2}{\mathrm{d}r^2}V_{ij}^{SR}(r)\right)_{r=r_0}, \tag{B.14}$$

$$A_2 = A_{ii} = A_{jj} = L'\left(\frac{\mathrm{d}^2}{\mathrm{d}r^2}V_{ii}^{SR}(r) + \frac{\mathrm{d}^2}{\mathrm{d}r^2}V_{jj}^{SR}(r)\right)_{r=r_0}, \tag{B.15}$$

$$B_1 = B_{ij} = \frac{L'}{a}\left(\frac{\mathrm{d}}{\mathrm{d}r}V_{ij}^{SR}(r)\right)_{r=r_0}, \tag{B.16}$$

$$B_2 = B_{ii} = B_{jj} = \frac{L'}{a}\left(\frac{\mathrm{d}}{\mathrm{d}r}V_{ii}^{SR}(r) + \frac{\mathrm{d}}{\mathrm{d}r}V_{jj}^{SR}(r)\right)_{r=r_0}, \tag{B.17}$$

$$C_1 = C_{ij} = L'a\left(\frac{\mathrm{d}^3}{\mathrm{d}r^3}V_{ij}^{SR}(r)\right)_{r=r_0}, \tag{B.18}$$

$$C_2 = C_{ii} = C_{jj} = L'a\left(\frac{\mathrm{d}^3}{\mathrm{d}r^3}V_{ii}^{SR}(r) + \frac{\mathrm{d}^3}{\mathrm{d}r^3}V_{jj}^{SR}(r)\right)_{r=r_0}, \tag{B.19}$$

$$g = Z + 8f(r) \tag{B.20}$$

$$g_1 = r_o df(r) \tag{B.21}$$

$$g(2) = r_o ddf(r) \tag{B.22}$$

$$\nabla = \left[\frac{-7.5391Z(Z+8f(r_0))+(A_1-B_1)}{-3.141Z(Z+8f(r_0))+(A_1+2B_1)+21.765Zaf'(r_0)}\right], \tag{B.23}$$

$$B_{\mathrm{T}} = \tfrac{1}{3}(C_{11} + 2C_{12}) \tag{B.24}$$

with $L = (e^2/4a^4)$ and $L' = (4a^3/e^2)$, and

$$\sigma = \tfrac{1}{2}(C_{11} - C_{12}), \tag{B.25}$$

in the form of

$$V_{ij}^{SR}(r) = b\beta_{ij}\exp\left(\frac{r_i + r_j - r_{ij}}{\rho}\right) - \frac{c_{ij}}{r_{ij}^6} - \frac{d_{ij}}{r_{ij}^8}. \tag{B.26}$$

The short-range interaction energy is expressed in terms of the overlap repulsion (first term) and the vdW d–d and d–q attractions (second and third terms), respectively.

References

[1] Mujica A, Rubio Angel, Munoz A and Needs R J 2003 *Rev. Mod. Phys.* **75** 863

[2] Chantis A N, van Schilfgaarde M and Kotani T 2006 *Phys. Rev. Lett.* **96** 086405

[3] Belogorokhov A, Florentsev A, Belogorokhov I and Elyutin A 2006 *Phys. Solid State* **48** 637

[4] Jain M 1991 *Diluted Magnetic Semiconductors* (Singapore: World Scientific)

[5] Firszt F 1993 *Semicond. Sci. Technol.* **8** 721
Firszt F, Meczynska H, Sekulska B, Szatkowski J, Paszkowicz W and Kachniarz J 1995 *Semicond. Sci. Technol.* **10** 197
Paszkowicz W, Firszi F, Legowski S, Meczynska H, Zakrzewski J and Marczak M 2002 *Phys. Status Solidi* b **229** 57

[6] Peterson D L, Petrou A, Giriat W, Ramdas A K and Rodriguez S 1986 *Phys. Rev.* B **33** 1160

[7] Furdyna J K, Giriat W, Mitchell D F and Sproule G I 1983 *J. Solid State Chem.* **46** 349

[8] Arora A K, Suh E-K, Debska U and Ramdas A K 1988 *Phys. Rev.* B **37** 2927

[9] Lin C-M, Chuu D-S, Xu J-a, Huang E, Chou W-C, Hu J-Z and Pei J-H 1998 *Phys. Rev.* B **58** 16

[10] Lin C-M, Chuu D-S, Yang T-J, Chou W-C, Xu J-a and Huang E 1997 *Phys. Rev.* B **55** 13641
Lin C-M and Chuu D-S 2000 *Phys. Lett.* A **266** 435
Lin C-M and Chuu D-S 2001 *Physica* B **304** 221

[11] Karzel H, Potzel W, Köfferlein M, Schiessl W, Steiner M, Hiller U, Kalvius G M, Mitchell D W, Das T P, Blaha P, Schwarz K and Pasternak M P 1996 *Phys. Rev.* B **35** 11425

[12] Majewski A J and Vogl P 1987 *Phys. Rev.* B **35** 9666

[13] Andreoni W and Maschke K 1980 *Phys. Rev.* B **22** 4816

[14] Chelikowsky J R 1987 *Phys. Rev.* B **35** 1174

[15] Zhang S B and Cohen M L 1987 *Phys. Rev.* B **35** 7604

[16] Löwdin P O 1956 *Adv. Phys.* **5** 1
Löwdin P O 1947 *Ark. Mat. Astr. Fys. (Sweden)* **35A** 30

[17] Lundqvist S O 1957 *Ark. Fys. (Sweden)* **12** 365

[18] Singh R K 1982 *Phys. Rep. (The Netherlands)* **85** 259–401

[19] Sörgel J and Scherz U 1998 *Eur. Phys. J.* B **5** 45

[20] Mayanovic R A, Sladek R J and Debska U 1988 *Phys. Rev.* B **38** 1311

[21] Cochran W 1971 *CRC Crit. Rev. Solid State Sci.* **2** 1

[22] Huggins M L and Sakamoto Y 1957 *J. Phys. Soc. Japan* **12** 241
Huntington H B 1958 *Solid State Phys.* **7** 214
Tosi M P 1964 *Solid State Phys.* **16** 1

[23] Hafemeister D W and Flygare W H 1965 *J. Chem. Phys.* **43** 795

[24] Slater J C and Kirkwood J G 1931 *Phys. Rev.* **37** 682

[25] Varshney D, Kaurav N, Sharma P, Shah S and Singh R K 2004 *Phase Transit.* **77** 1075
Varshney D, Sharma P, Kaurav N, Shah S and Singh R K 2004 *Phys. Status Solidi* b **241** 3374
Varshney D, Kinge R, Sharma P, Kaurav N and Singh R K 2005 *Indian J. Pure Appl. Phys.* **43** 939

[26] Tessmai J R, Kahn A K and Shocklry W 1953 *Phys. Rev.* **92** 890

[27] Euiot R J and Leath R A 1976 *Dynamical Properties of Solids* vol II, ed G K Horton and A A Maraduddin (New York: Academic) p 386

[28] Vegard L 1921 *Z. Phys.* B **5** 17

[29] Lide D R (ed) 1999 *CRC Handbook of Chemistry and Physics* 79th edn (New York: CRC Press)

[30] Gray D E (ed) 1963 *American Institute of Physics Handbook* (New York: McGraw Hill)

[31] Abrikosov N Kh, Bankina V F, Poretskaya L V, Sheliniova L E and Shudnova E V 1969 *Semiconducting II–VI and V–VI Compounds* (New York: Plenum)

[32] Lee B H 1970 *J. Appl. Phys.* **41** 2988

[33] Van Vechten J A 1973 *Phys. Rev.* B **7** 1479

[34] Murnaghan F D 1944 *Proc. Natl Acad. Sci. USA* **3** 244

[35] Miller A J, Saunders G A and Yogurtcu Y K 1981 *Phil. Mag.* A **43** 1447
Miller A J, Saunders G A and Yogurtcu Y K 1981 *J. Phys. Chem. Solids* **42** 49
Miller A J, Saunders G A and Yogurtcu Y K 1982 *J. Phys. C: Solid State Phys.* **15** 657

[36] Born M and Huang K 1956 *Dynamical Theory of Crystal Lattice* (Oxford: Clarendon)

[37] Vukcevich M R 1972 *Phys. Status Solidi* b **54** 435

[38] Varshney D, Kaurav N, Kinge R and Singh R K 2007 *J. Phys.: Condens. Matter* **19** 346 212
Varshney D, Kaurav N, Kinge R and Singh R K 2007 *J. Phys.: Condens. Matter* **19** 236204
Vaitheeswaran G, Kanchana V, Heathman S, Idiri M, Le Bihan T, Svane A, Delin A and Johansson B 2007 *Phys. Rev.* B **75** 184108
Varshney D, Kinge R, Kaurav N, Choudhary K K and Singh R K 2006 *Am. Inst. Phys Pub.* **850** 1301
Varshney D, Kaurav N, Kinge R, Shah S and Singh R K 2005 *High Pressure Res.* **25** 145
Varshney D, Kaurav N, Sharma P, Shah Sanjay and Singh R K 2004 *Phys. Status Solidi* b **241** 3179

[39] Varshney D, Sharma P, Kaurav N, Shah S and Singh R K 2005 *J. Phys. Soc. Japan* **74** 382
Varshney D, Kaurav N, Sharma P, Shah S and Singh R K 2004 *Phys. Status Solidi* b **241** 3374
Varshney D, Sharma P, Kaurav N and Singh R K 2005 *Bull. Mater. Sci.* **28** 651

[40] Varshney D, Kaurav N, Sharma U and Singh R K 2008 *J. Alloys Compounds* **448** 250

[41] Varshney D, Kaurav N, Kinge R and Singh R K 2008 *Phase Transit.* **81** 1
Varshney D, Kaurav N, Kinge R and Singh R K 2008 *J. Phys. Chem. Solids* **69** 60
Varshney D, Kaurav N, Kinge R and Singh R K 2007 *Comput. Mater. Sci.* at press doi:10.1016/j.commatsci. 2007.05.009